X-ray magnetic circular dichroism in UGe_2: first-principles calculations

2007 J. Phys.: Condens. Matter 19 186222

(http://iopscience.iop.org/0953-8984/19/18/186222)

IOP PUBLISHING JOURNAL OF PHYSICS: CONDENSED MATTER

J. Phys.: Condens. Matter **19** (2007) 186222 (10pp) doi:10.1088/0953-8984/19/18/186222

X-ray magnetic circular dichroism in UGe_2: first-principles calculations

V N Antonov[1,2,3], B N Harmon[1] and A N Yaresko[2]

[1] Ames Laboratory, Iowa State University, IA 50011, USA
[2] Max Planck Institute for Physics of Complex Systems, Dresden D-01187, Germany

Received 1 December 2006, in final form 12 February 2007
Published 13 April 2007
Online at stacks.iop.org/JPhysCM/19/186222

Abstract

The electronic structure and x-ray magnetic circular dichroism (XMCD) spectra of UGe_2 at the U $N_{4,5}$, $N_{2,3}$ and Ge K and $L_{2,3}$ edges are investigated theoretically from first principles, using the fully relativistic spin-polarized Dirac linear muffin-tin orbital (LMTO) band structure method. The electronic structure is obtained with the local spin-density approximation (LSDA), as well as the LSDA + U method. The origin of the XMCD spectra in the compound is examined.

(Some figures in this article are in colour only in the electronic version)

1. Introduction

The coexistence of ferromagnetism (FM) and superconductivity (SC) has been at the forefront of condensed matter research since a pioneering paper by Ginzburg [1]. The interplay between two long-range orderings FM and SC is a fascinating aspect in strongly correlated electron systems because generally SC does not favourably coexist with FM since the FM moment gives rise to an internal magnetic field, which breaks the pairing state.

During the last three decades, however, the discovery of a number of magnetic superconductors has allowed for a better understanding of how magnetic order and superconductivity can coexist. It seems to be generally accepted that antiferromagnetism with local moments coming from rare-earth elements readily coexists with type-II superconductivity [2]. This is because superconductivity and magnetism are carried by different types of electrons; magnetism is connected with deeply seated 4f electrons, while superconductivity is fundamentally related to the outermost electrons such as s, p, and d electrons. In the case of a ferromagnetic superconductor the situation is more complex, because internal fields are not cancelled out in the range of a superconducting coherence length, in contrast with an antiferromagnetic superconductor.

[3] Permanent address: Institute of Metal Physics, Vernadsky Street, 03142 Kiev, Ukraine.

Recently, UGe_2 has attracted considerable attention, because the coexistence of SC and FM was found under high pressure [3, 4]. It is particularly interesting to note that both ferromagnetism and superconductivity may be carried by itinerant 5f electrons, which can be homogeneously spread in real space, although this is still a matter of debate and remains to be resolved.

UGe_2 crystallizes in the orthorhombic $ZrGa_2$ structure (space group $Cmmm$). At ambient pressure, UGe_2 orders ferromagnetically below the Curie temperature $T_C = 52$ K with an ordered moment of 1.4 μ_B. The magnetic properties are strongly anisotropic, and the easy magnetization axis is the crystallographic a-axis of the $ZrGa_2$ structure. Superconductivity is found in the pressure range 1.0–1.6 GPa. The highest superconducting critical temperature T_{SC} is 0.8 K at a pressure P_C of 1.2 GPa, while T_C is 35 K at that pressure. As the applied pressure increases, the superconductivity disappears where the ferromagnetism disappears at around 1.7 GPa. Therefore, the superconductivity and ferromagnetism in UGe_2 seem to be closely related, although the mechanism of superconductivity has not been understood yet, and it is very important to characterize the magnetic properties of UGe_2. The XMCD technique developed in recent years has evolved into a powerful magnetometry tool to separate orbital and spin contributions to element-specific magnetic moments. XMCD experiments measure the absorption of x-rays with opposite (left and right) states of circular polarization.

Study of the 5f electron shell in uranium compounds is usually performed by tuning the energy of the x-ray close to the $M_{4,5}$ edges of uranium, where electronic dipole transitions between $3d_{3/2,5/2}$ and $5f_{5/2,7/2}$ states occur. There are some features in common for all the uranium compounds that have been investigated up to now. First, the dichroism at the M_4 edge is much larger, sometimes one order of magnitude larger, than at the M_5 edge. Second, the dichroism at the M_4 edge has a single negative lobe that has no distinct structure; on the other hand, two lobes, a positive and a negative one, are observed at the M_5 edge. Concerning the line shape of the XMCD signal, the investigated metallic uranium compounds fall into two types according to the relative intensity of the positive and negative lobes observed at the M_5 edge. The two lobes have almost equal intensity for UP_3, UPd_2Al_3, UPtAl, and UBe_{13}. On the other hand, the positive lobe is smaller in comparison with the negative lobe for US, $USb_{0.5}Te_{0.5}$, UFe_2, URu_2Si_2, UCoAl, and URhAl [5]. The appearance of two lobes is a finger-print of (i) an appreciable density of empty $j = 7/2$ sublevels with both negative and positive $m_{7/2}$ and (ii) a sufficient energy spread over these sublevels [6, 7].

In a recent publication [8] we reported on x-ray absorption and magnetic circular dichroism measurements performed at the $M_{4,5}$ edges of uranium in the ferromagnetic superconductor UGe_2. The spectra are described well by the LSDA + U electronic structure computation method. Combined with the analysis of the published (i) x-ray photoemission spectrum, (ii) two-dimensional electron positron momentum density, and (iii) angular dependence of the de Haas van Alphen frequencies, we infer $U = 2$ eV for the Coulomb repulsion energy within the 5f electron shell.

The present work is an extension of the previous study. Recently, Okane *et al* [9] measured x-ray absorption magnetic circular dichroism at the U $N_{4,5}$ and $N_{2,3}$ edges as well as at the Ge $L_{2,3}$ edges for the ferromagnetic superconductor UGe_2 in the normal state. The orbital and spin magnetic moments deduced from the sum rule analysis of the XMCD data indicate that the U atom in UGe_2 is considered to be closer to the trivalent state rather than the tetravalent state. The XMCD measurement at the U $N_{2,3}$ indicates that the U 6d electrons have negligibly small magnetic contributions.

Inada *et al* [10] also performed XMCD experiments at the Ge K edge in UGe_2. The Ge K edge XMCD spectrum shows a main negative peak near the edge and a small positive one at 7 eV above the edge. The amplitude of this spectrum is unusually very large, in spite of being at ligand sites.

The aim of this work is the theoretical study of the XMCD spectra of UGe_2 at the U $N_{4,5}$, $N_{2,3}$ and Ge K and $L_{2,3}$ edges. The paper is organized as follows. Section 2 presents a description of the computational details. Section 3 is devoted to the XMCD properties of the UGe_2 calculated in the LSDA and LSDA + U approximations. The XMCD theoretical calculations are compared with the experimental measurements. Finally, the results are summarized in section 4.

2. Computational details

The details of the computational method are described in our previous papers [5, 11, 8], and here we only mention several aspects. The calculations have been performed for the orthorhombic $ZrGa_2$ structure (space group *Cmmm*) [12] with lattice constants $a = 4.0089$ Å, $b = 15.0889$ Å and $c = 4.095$ Å using the spin-polarized linear muffin-tin orbital (LMTO) method [13, 14] with the combined correction term taken into account. We used the Perdew–Wang [15] parametrization for the exchange–correlation potential. Brillouin zone (BZ) integrations were performed using the improved tetrahedron method [16] and charge was obtained self-consistently with 657 irreducible **k**-points. To improve the potential, we include additional empty spheres. The basis consisted of U s, p, d and f; Ge s, p, and d; and empty spheres s, and p LMTOs.

The U $N_{4,5}$, $N_{2,3}$ and Ge K and $L_{2,3}$ XMCD spectra have been calculated with the magnetization along the a-axis, which is the easy axis in UGe_2. The intrinsic broadening mechanisms have been accounted for by folding XMCD spectra with a Lorentzian. For the finite lifetime of the core hole, a constant width Γ_c, in general from [17], has been used. The finite apparative resolution of the spectrometer has been accounted for by a Gaussian of 0.6 eV. In order to simplify the comparison of the theoretical x-ray isotropic absorption spectra of UGe_2 to the experimental spectra, we take into account the background intensity, which affects the high-energy part of the spectra and are caused by different kinds of inelastic scattering of the electron promoted to the conduction band above the Fermi level due to x-ray absorption (scattering on the potentials of surrounding atoms, defects, phonons etc). To calculate the background spectra, we used the model proposed by Richtmyer *et al* [18] (for details, see [19]).

We have adopted the LSDA + U method [20] as a different level of approximation to treat the electron–electron correlation. We used the rotationally invariant LSDA + U method. This method is described in detail in our previous paper [21]. The effective on-site Coulomb repulsion U was considered as an adjustable parameter, and its value was refined by comparing calculated results to available experimental data. In our previous paper [8] the calculations were performed for U varying from 0.5 to 4.0 eV with a 0.5 eV increment. It was found that the results with $U = 2$ eV give a more consistent interpretation of the whole complex of experimental data. This value has been chosen in the present calculations. For the exchange integral J, a value of 0.5 eV estimated from constrained LSDA calculations was used.

3. Results and discussion

3.1. U $N_{4,5}$ XMCD spectra

Figure 1 shows the calculated XAS and XMCD spectra in the LSDA and LSDA + U approximations for UGe_2 at the $N_{4,5}$ edges together with the corresponding experimental data [9]. The experimentally measured XAS spectra have a rather simple line shape composed of two white line peaks at the N_5, and N_4 edges and no distinct fine structures due to multiplet splitting were observed. This justifies the description of the absorption of the incident x-rays in terms of a one-particle approximation. Hence, valuable information on the nature of the

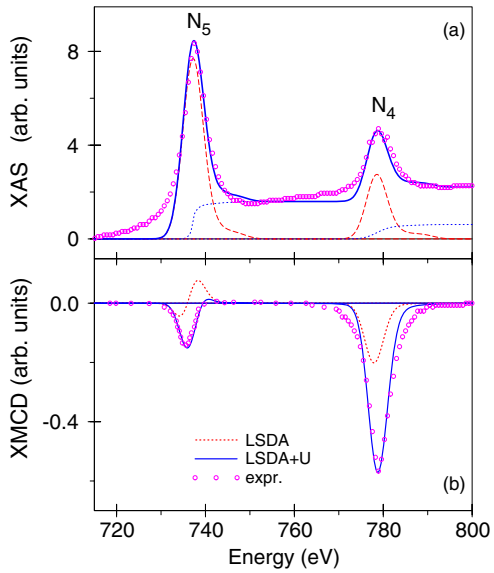

Figure 1. (a) Theoretically calculated (dashed line) and experimental [9] (circles) isotropic absorption spectra of UGe_2 at the U $N_{4,5}$ edges. Experimental spectra were measured with an external magnetic field (2 T) at 25 K. Dotted lines show the theoretically calculated background spectra; full thick lines are the sum of the theoretical XAS and background spectra. (b) Experimental [9] (circles) XMCD spectra of UGe_2 at the U $N_{4,5}$ edges in comparison with theoretically calculated spectra using the LSDA (dotted line) and LSDA + U (full line) approximations.

5f electrons can be obtained from the comparison of experimental data to the results of band-structure calculations.

The XMCD signals at the N_5 and N_4 edges have the same sign, and the XMCD signals at the N_4 edge have a much higher intensity than those at the N_5 edge. These behaviours were commonly observed in the XMCD spectra at the U $M_{4,5}$ edges of the ferromagnetic uranium compounds [5], from which one can conclude that the orbital and the spin magnetic moments are directed in opposite directions to each other.

A qualitative explanation of the XMCD spectra shape is provided by analysis of the orbital character, occupation numbers of individual 5f orbitals and corresponding selection rules. Because of the electric dipole selection rules ($\Delta l = \pm 1$; $\Delta j = 0, \pm 1$), the major contribution to the absorption at the N_4 edge stems from the transitions $4d_{3/2} \rightarrow 5f_{5/2}$ and that at the N_5 edge originates primarily from $4d_{5/2} \rightarrow 5f_{7/2}$ transitions, with a weaker contribution from $4d_{5/2} \rightarrow 5f_{5/2}$ transitions. The selection rules for the magnetic quantum number m_j (m_j is restricted to $-j, \ldots +j$) are $\Delta m_j = +1$ for the left polarization of the photon with respect to the magnetization direction ($\lambda = +$) and $\Delta m_j = -1$ for the right polarization ($\lambda = -$).

In our previous paper [22] we showed that, qualitatively, the XMCD spectrum of U at the M_5 edge ($I = \mu^- - \mu^+$) can be represented roughly by the following m_j projected partial density of states (DOS): $[N^{7/2}_{-7/2} + N^{7/2}_{-5/2}] - [N^{7/2}_{7/2} + N^{7/2}_{5/2}]$. Here we used the notation $N^j_{m_j}$ with the total momentum j and its projection m_j. As a result, the shape of the M_5 XMCD spectrum usually results in two peaks of opposite sign—a negative peak at lower energy and a positive peak at higher energy. The relative intensity of the negative and positive lobes depends on the value of the crystal field and Zeeman splitting of the $5f_{7/2}$ electronic states [7]. As the separation of the peaks is smaller than the typical lifetime broadening, the peaks cancel each

other to a large extent, thus leading to a rather small signal. Similar consideration is valid also for the N_5 edge.

It can be shown (see [22]) that the XMCD spectrum of U at the M_4 and N_4 edges can be represented fairly well by considering the m_j projected partial density of states: $-[N_{3/2}^{5/2} + N_{5/2}^{5/2}]$. This explains why the dichroic M_4 as well as the N_4 lines in uranium compounds consist of a single, nearly symmetric negative peak.

We should note, however, that the explanation for the XMCD line shape in the terms of partial DOSs presented above should be considered only qualitatively. First, there is no full compensation between transitions with equal final states due to a difference in the angular matrix elements; second, in our consideration we neglect cross terms in the transition matrix elements. Besides, here we have used the jj-coupling scheme, where the total momentum $\mathbf{j}$ is written as $\mathbf{j} = \mathbf{l} + \mathbf{s}$. However, the combination of the hybridization, Coulomb, exchange and crystal-field energies may be so large relative to the 5f spin–orbit energy that the jj-coupling is no longer an adequate approximation.

Figure 1(b) shows the calculated XMCD spectra in the LSDA and LSDA + U approximations for UGe_2, together with the corresponding experimental data [9]. The overall shapes of the calculated and experimental uranium $N_{4,5}$ XMCD spectra correspond well to each other. The major discrepancy between the calculated and experimental XMCD spectra is the size of the N_4 XMCD peak. The LSDA theory produces a much smaller intensity for the XMCD spectrum at the N_4 edge in comparison with the experiment. It also cannot produce the correct shape for the N_5 XMCD spectrum. On the other hand, the LSDA + U approximation with $U = 2$ eV produces excellent agreement in the shape and intensity of XMCD spectra at the $N_{4,5}$ edges.

Now we focus on values of moments of the 5f shell. The orbital magnetic moment can be estimated from the XMCD sum rules [23, 24]. By integrating the experimentally measured XAS and XMCD spectra at the $M_{4,5}$ edges, we obtained $\mu_L = 1.91$ and 1.75 μ_B for the hypothetical f^2 and f^3 configurations, respectively [8]. A similar procedure has been used by Okane *et al* at the $N_{4,5}$ edges [9]; they obtained $\mu_L = 1.89$ and 2.35 μ_B for the f^2 and f^3 configurations, respectively. Although the values for the f^2 configuration are very close, the values for the f^3 configuration differ by more than 30%. One of the possible reasons for such disagreement might be connected with the fact that the application of the sum rule is valid only when the spin–orbit splitting of the core level is sufficiently large compared with other interactions, including the core-valence Coulomb and exchange interaction. The condition may not be so clear at the U $N_{4,5}$ edges, because the spin–orbit splitting is considerably smaller than that at the U $M_{4,5}$ edges [9]. One should also mention that XMCD sum rules are derived within an ionic model using a number of approximations [5, 25]. The largest mistake comes from ignorance of the energy dependence of the radial matrix elements in sum rules; sometimes it can produce an error of up to 100% [19].

From our LSDA + U band-structure calculations with $U = 2$ eV we obtain a larger 5f orbital magnetic moment: $M_L = 3.46\ \mu_B$, which may indicate that the LSDA + U is producing too much localization for the 5f orbitals [21].

The analysis of the orbital projected DOS provided in our previous paper shows that, for $U = 2$ eV, the two most populated 5f orbitals become almost completely occupied and the corresponding peaks of the orbital resolved DOS are found below the Fermi energy, E_F (see figure 3 in [8]). The third most occupied orbital remains only partially occupied. Whereas the main peak of the DOS projected onto this orbital is situated below E_F, an additional narrow peak can be seen just above the Fermi level. Even for $U = 4$ eV, the third peak remains partially occupied. We can conclude that the U atom in UGe_2 possesses a valency somewhat in between U^{4+} (f^2) and U^{3+} (f^3).

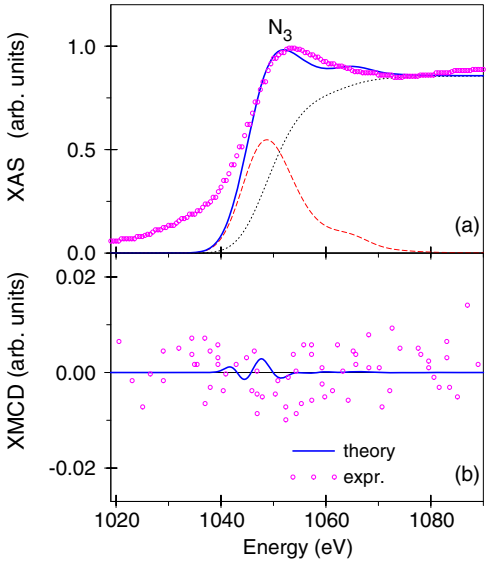

Figure 2. (a) Theoretically calculated (dashed line) and experimental [9] (circles) isotropic absorption spectra of UGe_2 at the U N_3 edge. Dotted lines show the theoretically calculated background spectrum; the full thick line is the sum of the theoretical XAS and the background spectrum. (b) Experimental [9] (circles) XMCD spectrum of UGe_2 at the U N_3 edge in comparison with theoretically calculated spectra using the LSDA + U approximations (full line).

One should mention that the ratio $R = -\mu_L/\mu_S$ of the orbital to spin moment is not in disagreement with the experiment: our LSDA + U calculations produce $R = 2.25$, while the experimental estimations give 2.24 and 2.51 for f^3 configurations by integrating the spectra at the $M_{4,5}$ and $N_{4,5}$ edges, respectively [8, 9].

3.2. U $N_{2,3}$ and Ge $L_{2,3}$ XMCD spectra

In order to investigate the contribution of the U 6d electrons to the magnetization, Okane *et al* [9] measured XMCD at the U $N_{2,3}$ edges too. Figure 2 shows the calculated XAS and XMCD spectra in the LSDA + U approximations for UGe_2 at the N_3 edge together with the corresponding experimental data [9]. The experimentally measured XAS spectrum has quite a large background intensity. One can see that no appreciable XMCD signals are observed at the U N_3 edge.

The theoretical LSDA + U calculations also produce an XMCD spectrum of very small intensity; figure 2(b). This might be connected with quite a small U 6d spin and orbital magnetic moments equal to 0.075 and -0.041 μ_B, respectively.

Okane *et al* also measured XAS and XMCD spectra in the region of the Ge $L_{2,3}$ absorption edges [9]. The spectra have quite complicated line shapes and it is hard to separate the Ge $L_{2,3}$ signal from the U N_2 and Gd M_4 XMCD signals. The latter arises from the sample holder. Figure 3 presents the calculated XMCD spectra of the UGe_2 at the Ge $L_{2,3}$ edges compared with the experimental data [9]. The authors of [9] consider a positive peak B at 1215 eV, a negative peak C at 1228 and another negative peak D at 1255 eV as the XMCD spectra of the Ge $L_{2,3}$ edges, since the energy separation between those structures is close to the spin–orbit splitting of the Ge $L_{2,3}$ core level 30 eV. A strong negative peak at around 1183 eV (peak A) apparently comes from the Gd M_5 spectrum of the sample holder. A positive XMCD peak at

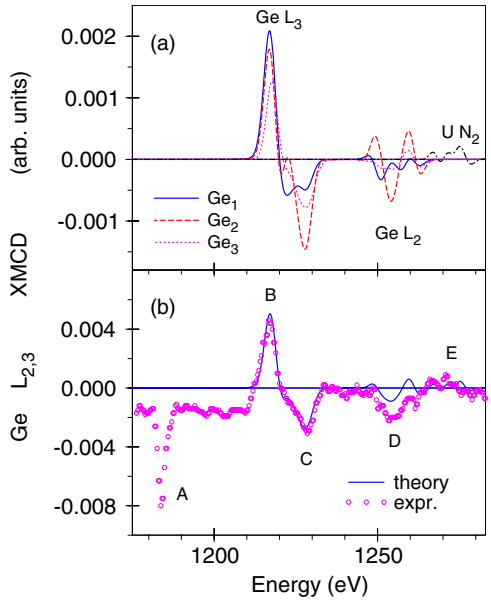

Figure 3. (a) Theoretically calculated XMCD spectra of UGe_2 at the U N_2 and Ge $L_{2,3}$ edges at different Ge sites. (b) Experimental [9] (circles) XMCD spectra of UGe_2 at the Ge $L_{2,3}$ and U N_2 edges in comparison with theoretically calculated spectra using the LSDA + U approximations (full line).

1215 eV may include probably not only the Ge L_3 contribution but also a contribution from Gd M_4, and the broad hump at around 1270 eV may arise from U N_2 contributions [9].

Our band-structure calculations perfectly describe the peaks B and C as the L_3 XMCD spectrum, while the L_2 XMCD spectrum reproduces the fine structure *D* well. Due to larger U $4p_{1/2}$ electron energy binding in comparison with the Ge $2p_{1/2}$ electron energy binding, the U N_2 XMCD spectrum is situated at the higher-energy side of the Ge L_2 spectrum (peak *E*). The values of Gd 5d orbital (spin) magnetic moments are equal to 0.018 (0.019), 0.022 (0.013) and 0.010 (0.011) μ_B at the Ge_1, Ge_2 and Ge_3 sites, respectively. The main contribution to the intensity of XMCD $L_{2,3}$ spectra comes from Ge_1 and Ge_2 sites, because they have larger magnitudes for their spin and orbital polarizations (figure 3(a)).

Through turning the spin–orbit interaction (SOI) off separately on the Ge 4d and U 5f states, we found that the negative peak C originates from the spin polarization in the Ge 4d symmetric states through the SOI, while the Ge 4d and U 5f hybridization is responsible for the large positive XMCD at around 1215 eV (peak B).

One should mention that XMCD spectra at the U $N_{2,3}$ and Ge $L_{2,3}$ edges are mostly determined by the strength of the SO coupling of the initial U 4p and Ge 2p core states and spin-polarization of the final empty $d_{3/2,5/2}$ states while the exchange splitting of the U 4p and Ge 2p core states as well as the spin–orbit (SO) coupling of the d valence states are of minor importance for the XMCD at the U $N_{2,3}$ and Ge $L_{2,3}$ edges of UGe_2.

3.3. Ge K XMCD spectrum

The 4p states in transition metals usually attract only minor interest, because they are not the states responsible for magnetic or orbital orders. Recently, however, understanding 4p states has become important since XMCD spectroscopy using K edges of transition metals

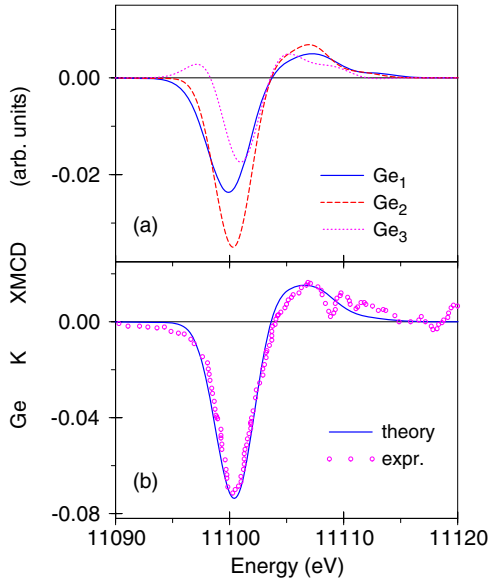

Figure 4. (a) Theoretically calculated XMCD spectra of UGe_2 at the K edge at different Ge sites; (b) theoretically calculated XMCD spectrum of UGe_2 at the Ge K edge using the LSDA + U approximations (full line) in comparison with the experimental spectra [10] (circles). The experimental spectrum was measured at 3 K with an external magnetic field (0.5 T) applied along the a-axis.

became popular, in which the 1s core electrons are excited to the 4p states through the dipolar transition. The K edge XMCD is sensitive to electronic states at neighbouring sites, because of the delocalized nature of the 4p states. It is expected that the ligand site XMCD is a candidate for one of the effective probes which can detect the mixing between p and f states in uranium compounds.

Figure 4(b) shows the calculated XMCD spectra in the LSDA + U approximation for UGe_2 at the K edge, together with the corresponding experimental data [10]. The experimental XMCD spectrum shows a main negative peak near 11 100 eV and a small positive peak at about 7 eV higher. One might expect only tiny signals of XMCD from the 4p band, because it does not possess a large magnetic moment. However, the intensity of the negative peak of the UGe_2 K XMCD spectrum reaches about 3% of the intensity of the fluorescence (or absorption) from the K edge [10]. This value is large. Even the iron K edge XMCD is only on the order of 0.3% [26].

The K XMCD spectra come from the orbital polarization in the empty p states, which may be induced by (1) the spin polarization in the p states through the SOI, and (2) the orbital polarization at neighbouring sites through hybridization.

We calculated the XMCD spectra at the Ge site by turning the SOI off separately on the Ge 4p and the U 5f states, respectively. We found that the prominent negative peak is reduced in intensity by more than one order of magnitude when the SOI on the U 5f states is turned off, while the small positive lobe almost does not change. When the SOI on the Ge 4p orbital is turned off, the negative prominent peak is slightly changed and the positive lobe is diminished. We can conclude that the positive lobe originates from the spin polarization in the Ge 4p symmetric states through the SOI. The Ge 4p and U 5f hybridization is responsible for large negative XMCD near the Ge K edge. This indicates that the Ge 4p orbital polarization

originates mainly from the large 5f orbital polarizations at neighbouring U atoms through Ge 4p–U 5f hybridization. This mechanism seems different from the XMCD in transition metal compounds, in which the 4p orbital polarization is induced mostly by the 4p spin polarization at the atom itself through the SOI [5].

Similar results have been obtained by Usuda *et al* [27] for the magnetic resonant x-ray scattering (MRXS) spectra at Ga sites in the antiferromagnetic cubic phase of UGa_3: the MRXS intensity largely decreased when the SOI on the U 5f states is turned off, while it was only slightly reduced when the SOI on the Ga 4p orbital is turned off.

From our LSDA + U band-structure calculations, the values of the orbital magnetic moment in the p projected bands are equal to -0.025, -0.031 and -0.006 μ_B at the Ge_1, Ge_2 and Ge_3 sites, respectively. The contributions to the intensity of the XMCD K spectrum from different Ge sites are related to the magnitude of their orbital polarizations (figure 4(a)).

4. Summary

We have studied, by means of an *ab initio* fully relativistic spin-polarized LMTO method, the x-ray magnetic circular dichroism in UGe_2 at the U $N_{4,5}$, $N_{2,3}$ and Ge K and $L_{2,3}$ edges.

The overall shapes of the calculated and experimental uranium $N_{4,5}$ XMCD spectra of UGe_2 correspond well to each other. The major discrepancy between the calculated and experimental XMCD spectra is the size of the N_4 XMCD peak. The LSDA theory produces a much smaller intensity for the XMCD spectrum at the N_4 edge in comparison with the experiment. It also does not produce the correct shape for the N_5 XMCD spectrum. On the other hand, the LSDA + U approximation produces excellent agreement in the shape and intensity of XMCD spectra at the $N_{4,5}$ edges.

The theoretical LSDA+U calculations produce an XMCD spectrum of very small intensity at the U N_3 edge in agreement with the experimental observation, in which no appreciable XMCD signals are observed. This might be connected to the quite small U 6d spin and orbital magnetic moments.

The Ge K edge XMCD spectrum shows a main negative peak near the edge and a small positive peak at 7 eV above the edge. The amplitude of this spectrum is unusually large, reaching about 3% of the intensity of the absorption. The K edge XMCD is sensitive to the electronic structure at neighbouring sites because of the delocalized nature of the 4p states. We found that the Ge 4p orbital polarization originates mainly from the large 5f orbital polarizations at neighbouring U atoms through the Ge 4p and U 5f hybridization, resulting in an unusual large XMCD signal at the Ge K edge.

Acknowledgments

This work was carried out at the Ames Laboratory, which is operated for the US Department of Energy by Iowa State University under contract no. DE-AC02-07CH11358. This work was supported by the Office of Basic Energy Sciences of the US Department of Energy.

V N Antonov gratefully acknowledges the hospitality at the Ames Laboratory during his stay.

References

[1] Ginzburg V L 1957 *Sov. Phys.—JETP* **4** 153

[2] Aso N, Motoyama G, Uwatoko Y, Ban S, Nakamura S, Nishioka T, Homma Y, Shiokawa Y, Hirota K and Sato N K 2006 *Phys. Rev.* B **73** 054512

[3] Saxena S *et al* 2000 *Nature* **406** 587
[4] Huxley A, Sheikin I, Ressouche E, Kernavanois N, Braithwaite D, Calemczuk R and Flouquet J 2001 *Phys. Rev.* B **63** 144519
[5] Antonov V, Harmon B and Yaresko A 2004 *Electronic Structure and Magneto-Optical Properties of Solids* (Dordrecht: Kluwer)
[6] de Reotier P D *et al* 1997 *J. Phys.: Condens. Matter* **9** 3291–6
[7] Antonov V N, Harmon B N, Andryushchenko O, Bekenev L and Yaresko A N 2004 *Low Temp. Phys.* **30** 411–26
[8] Yaresko A N, de Réotier P D, Yaouanc A, Kernavanois N, Sanchez J P, Menovsky A A and Antonov V N 2005 *J. Phys.: Condens. Matter* **17** 2443
[9] Okane T *et al* 2006 *J. Phys. Soc. Japan* **75** 024704
[10] Inadaa Y, Honmab T, Kawamurab N, Suzukib M, Miyagawab H, Yamamotoc E, Hagac Y, Okaned T, Fujimorid S and Onuki Y 2005 *Physica* B **359–361** 1054–6
[11] Antonov V N, Harmon B N and Yaresko A N 2001 *Phys. Rev.* B **64** 024402
[12] Oikawa K, Kamiyama T, Asano H, Onuki Y and Kohgi M 1996 *J. Phys. Soc. Japan* **65** 3229–32
[13] Andersen O K 1975 *Phys. Rev.* B **12** 3060
[14] Nemoshkalenko V V and Antonov V N 1998 *Computational Methods in Solid State Physics* (London: Gordon and Breach)
[15] Perdew J and Wang Y 1992 *Phys. Rev.* B **45** 13244–9
[16] Blöchl P E, Jepsen O and Andersen O K 1994 *Phys. Rev.* B **49** 16223
[17] Fuggle J C and Inglesfield J E 1992 *Unoccupied Electronic States* (*Springer Topics in Applied Physics* vol 69) (New York: Springer)
[18] Richtmyer F K, Barnes S W and Ramberg E 1934 *Phys. Rev.* **46** 843
[19] Antonov V N, Jepsen O, Yaresko A N and Shpak A P 2006 *J. Appl. Phys.* **100** 043711
[20] Anisimov V I, Zaanen J and Andersen O K 1991 *Phys. Rev.* B **44** 943
[21] Yaresko A N, Antonov V N and Fulde P 2003 *Phys. Rev.* B **67** 155103
[22] Antonov V N, Harmon B N and Yaresko A N 2003 *Phys. Rev.* B **68** 214424
[23] Thole B T, Carra P, Sette F and van der Laan G 1992 *Phys. Rev. Lett.* **68** 1943
[24] van der Laan G and Thole B T 1996 *Phys. Rev.* B **53** 14458
[25] Ebert H 1996 *Rep. Prog. Phys.* **59** 1665–735
[26] Maruyama H *et al* 1999 *J. Synchrotron Radiat.* **6** 1133–7
[27] Usuda M, Igarashi J and Kodama A 2004 *Phys. Rev.* B **69** 224402